



Integrated 3D printed scaffolds and electrical stimulation for enhancing primary human cardiomyocyte cultures

Scott D. Adams^a, Ajay Ashok^b, Rupinder K. Kanwar^c, Jagat R. Kanwar^c, Abbas Z. Kouzani^{a,*}

^a School of Engineering, Deakin University, Geelong VIC 3216, Australia

^b Department of Pathology, Case Western Reserve University, Cleveland, OH 44106-7288, USA

^c Nanomedicine-Laboratory of Immunology & Molecular Biomedical Research, School of Medicine, Centre for Molecular and Medical Research, Deakin University, Waurn Ponds, VIC 3216, Australia

ARTICLE INFO

Keywords:

3D printing
Cell culture
Bioprinting
Scaffold
Electrical stimulation
Wireless
Cardiomyocytes

ABSTRACT

3D printing technology is driving innovation in a wide variety of disciplines, and is beginning to make inroads into the fields of medicine and biology. In particular, 3D printing is being increasingly utilized for the design and fabrication of three-dimensional cell culture scaffolds. This technology allows for scaffolds to be produced rapidly while maintaining a great deal of control over the matrix architecture. This paper presents an effective technique for rapidly designing and fabricating scaffolds from silicone rubber and polycaprolactone (PCL), appropriate for primary human cardiomyocyte cell cultures. Additionally, a stimulation device is developed and presented which can provide 6 channels of wirelessly controlled electrical stimulation to the cell culture scaffolds. The design, fabrication, benchtop evaluation, and biological evaluation of the scaffolds and stimulation device for primary human cardiomyocyte cell culture are presented. The results clearly indicate the effectiveness of both the scaffold fabrication technique and the operation of the stimulation device. The silicone rubber scaffold showed significantly lower cell attachment as compared to the PCL scaffold, validating the suitability of PCL as a material to be employed in the synthesis of bioscaffolds, employed in the management of several medical pathologies such as tissue regeneration and wound healing. Additionally, the biocompatible PCL scaffold stimulated with electrical impulse (5 V, 2 ms pulses, 1 Hz) exhibited higher cell attachment and differentiated actin cytoskeletal structures as compared to the unstimulated scaffold, indicating the potential of this technique in tissue engineering applications.

1. Introduction

Modern 3D printing technology is driving innovation in several fields including art, manufacturing and medicine [1]. Recently, 3D printing has begun to enter the field of regenerative medicine, through the production of intricate 3D objects fabricated from biocompatible materials, integrated with live biological cells [2]. This biological printing or bioprinting, has already shown significant potential in regenerative medicine and tissue engineering, facilitating the production or repair of: cartilage [3,4], bone [5], skin [6], vascular grafts [7], and many more [2].

Bioprinting has shown significant potential for rapid design and fabrication of cell culture scaffolds. A cell culture scaffold is a porous three-dimensional structure produced from a biocompatible material to enable controlled tissue development. This development is controlled through a number of features of the scaffold such as material selection, pore size, pore geometry and material biodegradability, which need to

be optimised to facilitate the required growth characteristics [8]. Using bioprinting to fabricate these scaffolds has significant advantages over many of the conventional techniques, such as particulate leaching, solvent casting, or gas foaming. 3D bioprinting allows for scaffolds to be produced rapidly in a highly repeatable manner while maintaining a great deal of control over the scaffold matrix architecture, and allows for the production of scaffolds with precise pore size, pore geometry and high levels of mechanical strength [8]. Use of the bioprinting technique also allows researchers to carry out the scaffold design, fabrication, and optimisation by themselves, with only minimal training.

One area of particular interest for these bioprinted constructs is to assist in the repair of myocardium, which gets damaged during a myocardial infarction (MI), commonly known as heart attack [9]. During MI, a significant number of cardiomyocytes can die (apoptosis) due to ischemia. As these cells are terminally differentiated with minimal regenerative efficacy, noncontracting fibrotic scars can devel-

* Corresponding author.

E-mail address: kouzani@deakin.edu.au (A.Z. Kouzani).

op, which can lead to a secondary potentially fatal MI and heart failure [10]. One method for avoiding a subsequent MI is to employ cellular cardiomyoplasty to regenerate the damaged myocardial tissue [11]. Cellular cardiomyoplasty is the implantation of in-vitro cultured cardiomyocytes into the damaged myocardium, to facilitate regeneration. However, these directly injected cardiomyocytes experience low cell retention and viability [12]. In order to address this issue of low cell viability, Christman, et al. [13] explored the use of a cell culture scaffold fabricated from fibrin sealant which could replace traditional cellular cardiomyoplasty. Their study found that this method considerably increased cell transport survival as it gave a temporary extracellular matrix to the injected cells. However, they learnt that the fibrin scaffold did not enhance cell retention [13].

As the heart is the largest physiological source of bioelectrical energy [14], a number of studies have investigated the effects of integrating electrical field stimulation into cardiac cell cultures. These studies have found that electrical stimulation can promote maturation, synchronous construct contractions, and the ultra-structural organization of cardiomyocytes derived from embryonic stem cells [15–21]. This stimulation is applied through a stimulation device interfaced with a desktop computer, used to control the stimulation [22].

The novelty of the research presented in this paper is two-fold. First, in relation to the 3D bioprinting aspect, this research offers an effective technique for rapidly designing and fabricating scaffolds appropriate for primary human cardiomyocyte (pHCM) cell cultures, from two different materials. Silicone rubber and Polycaprolactone (PCL) were investigated as scaffold materials due to their inherent biocompatibility and suitability as printing materials. The design, fabrication, and evaluation of the scaffolds as structures for culturing pHCM is presented in this paper.

Secondly, with regards to the electrical stimulation aspect, this research offers a low-cost, small footprint, highly customisable scaffold stimulation system as a proof of concept study. This system can be controlled in an entirely wireless manner without a desktop computer, unlike existing devices. This allows for the device to be placed directly within a cell culture cabinet and controlled without causing disruption to the cell culturing process. The design, fabrication, benchtop evaluation, and biological evaluation of this device are presented in this paper.

2. Materials and methods

2.1. Materials

Silicone rubber (Silcoferm S) (PCI Augsburg GmbH, Augsburg) with a density of 1.0 g/cm^3 and Polycaprolactone (PCL) (Sigma-Aldrich, St. Louis) with weight-average molecular weight (M_w) of $14,000 \text{ g/mol}$, density of 1.146 g/mL and were obtained as scaffold fabrication materials. 3 mm diameter graphite rods (Sigma-Aldrich, St. Louis) with trace metals basis of 99.995%, and platinum wire (Sigma-Aldrich, St. Louis) of diameter 0.25 mm, trace metal basis of 99.95% were obtained for constructing the stimulation system. Adult primary human cardiomyocytes (pHCM) obtained from Celprogen Inc. (San Pedro, CA) were employed throughout the study.

2.2. 3D bioprinting

The 3D cell culture scaffolds produced as part of this research were fabricated entirely on the EnvisionTEC 3D-Bioplotter, a rapid prototyping system which can fabricate complex three dimensional objects using custom materials. The 3D-Bioplotter uses an additive manufacturing process, where the object to be produced is sliced into layers of a fixed height, and each of these layers is printed sequentially. Each layer is produced by depositing material onto the print bed, through a pressure controlled syringe.

The EnvisionTEC 3D-Bioplotter allows for the production of objects

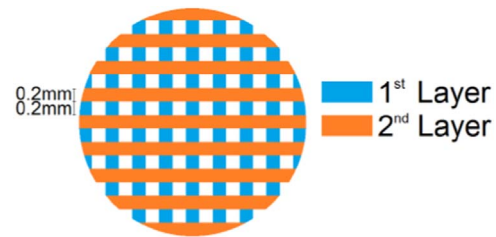


Fig. 1. Scaffold design (Top View).

from any materials with an appropriate viscosity. This device also can heat the material during the print process up to 250°C . Using this method of fabrication, cell culture scaffolds can be rapidly fabricated with uniform internal and external features.

2.3. Scaffold design

The scaffolds developed for this research were designed using the Solidworks 3D CAD software (Dassault Systèmes). In order for cell culturing to take place in a 48-well cell culture plate, the exterior surface of these scaffolds were designed as a square cuboid with length and width of 15 mm and height of 0.8 mm. This exterior design was converted to a Stereolithography (STL) file and imported to the EnvisionTEC Visual Machines software, for the design of the interior features. The interior of these scaffolds were designed as a matrix with an ideal porosity of 53%, with a strand size of $200 \mu\text{m}$, and $200 \mu\text{m}$ pores. A 2D representation of this interior structure can be seen in Fig. 1.

2.4. Scaffold fabrication

Two biocompatible materials were selected as suitable scaffold material candidates for testing. The first scaffold material was Silicone Rubber (PCI Augsburg GmbH, Augsburg), while the second material was polycaprolactone (PCL), a non-hazardous polymer used in a number of Food and Drug Authority (FDA) approved human implants [23]. These materials were selected for use due to their inherent biocompatibility, low cost, simple post-processing requirements and suitability for 3D printing. In addition to these shared properties, PCL is also a biodegradable material which has shown significant promise as a scaffold material for other cell types [24,25].

After optimising the printing parameters for each material, a number of scaffolds were fabricated using an EnvisionTEC Bioplotter (see Fig. 2). The printing parameters used in this study are shown in Table 1.

Excess material that was deposited on scaffold edges were removed with a scalpel, after which the scaffold had a length and width of 10 mm. A number (20) of these scaffolds were produced in order to verify the repeatability of the fabrication method. Fig. 2C shows the scaffolds within a 48-well cell culture plate for testing.

2.5. Electrical stimulation device

A custom, low cost, multi-channel device, was designed to provide regulated electrical stimulation to cell culture scaffolds. The outputs required for this device were determined through an investigation of the stimulation parameters used in previously published research. The studies suggested the following simulation parameters: voltage amplitude: 3–8 V, frequency: 1–4 Hz, and stimulation duration: 1–4 ms [17–21]. The device is designed such that a user can simultaneously stimulate multiple cell cultures, using any combination of these parameters. The device consists of the following components: micro-controller, voltage amplitude control circuitry, frequency and duration control circuitry, printed circuit board (PCB), Bluetooth transceiver, and control interface.

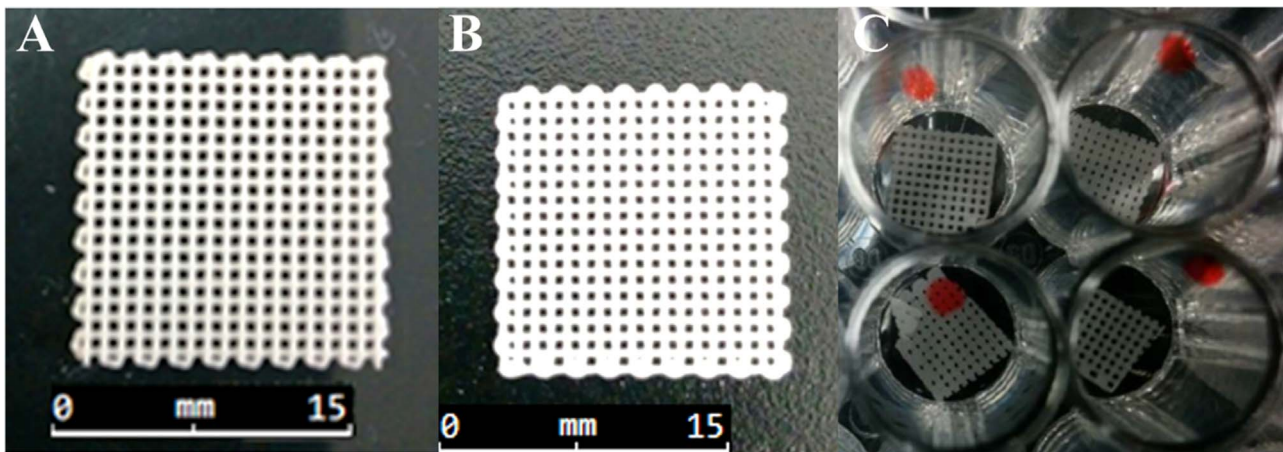


Fig. 2. (A) 3D printed Silicone rubber scaffold showing high levels of uniformity of the printed pores. (B) PCL scaffold showing high levels of uniformity of the printed pores. (C) PCL scaffolds placed in 48-well plate.

Table 1
EnvisionTEC 3D bioplotter print settings.

Material	Silicone	PCL
Temperature	8 °C	80 °C
Pressure	5 Bar	5.6 Bar
Speed	6.2 mm/s	4 mm/s
Pre flow delay	0.11 s	0 s
Post flow delay	−0.02 s	0 s
Time between layers	0 s	0 s
Minimum length	3 mm	3 mm
Cleaning interval	7 Layers	5 Layers

The microcontroller selected for this device is an Atmel ATmega88PA, which is a high performance, low power 8-bit microcontroller using the AVR enhanced reduced instruction set computing (RISC) architecture. This microcontroller was used to activate and control the output parameters of the stimulation channels. This was achieved using the integrated 8 and 16 bit timers to output pulse width modulated (PWM) signals from multiple microcontroller pins. This microcontroller was also used to read control signals from a Bluetooth transceiver connected to a smartphone application which was developed and used to control the stimulation.

In order to alter the amplitude of the output stimulation voltage, a novel circuit was developed which can produce a PWM controlled, regulated output voltage. To provide this adjustable voltage output, a voltage regulator is employed. The LM317 is an adjustable voltage regulator which can output over 1.5 A under operating conditions of 1.25 – 37 V. It has three terminals and features a typical line regulation of 0.01% and typical load regulation of 0.1%. When in a typical adjustable output configuration, the output voltage is governed according to $V_O = V_{REF}(1 + R_2/R_1) + V_2$. During operation, the LM317 develops a reference voltage of 1.25 V (V_{REF}) across R_1 (see Fig. 3). As both the reference voltage and the resistance R_1 are constant, the current (I_1) across the resistor R_2 is also constant. This indicates that the output voltage of the circuit can be adjusted through only altering the values of R_2 and V_2 . Therefore, if the potentiometer (R_2) is replaced with an adjustable voltage source with near zero impedance ($R_2 \approx 0$), the output voltage can be simply adjusted. The adjustable voltage source selected for this device was an operational amplifier configured as a non-inverting amplifier with a gain of 2, controlled by a smoothed 5 V PWM signal. This circuit design is illustrated in Fig. 3. In this configuration, the output voltage of the regulator can simply be controlled by altering the duty cycle of the PWM signal (d_{PWM}). The ideal output voltage can be calculated using $V_O = 1.25 V + 2(5 V \times d_{PWM})$.

In order to control the frequency and duration of the stimulation pulses, a high-side transistor based switching circuit was employed.

This circuit integrated a level switcher to allow a microcontroller output voltage of 5 V to be able to activate and deactivate the maximum output voltage of 8 V. Using a PWM signal as the input to this circuitry allowed for precise control of the stimulation pulse frequency and duration.

To secure the components of the stimulation device and to provide the appropriate electrical connections, two printed circuit boards were developed. The first PCB includes two channels of stimulation and utilises through-hole components. The second PCB includes 6 channels of stimulation and uses surface mounted components; the layout of this PCB is presented in Fig. 3B. After the fabrication of the PCBs, the electronic components of the stimulation device were assembled onto the board. To protect the device, it was placed within a plastic enclosure.

In order to control the stimulation device, a Bluetooth communication transceiver was added. Using a wireless technology such as Bluetooth allows for control over the stimulation device without having to physically enter the cell growth environment where the device is operating, reducing the contamination risk. To control the stimulation device, an Android application was developed. This application was used to activate or deactivate the stimulation on each channel, as well as alter the stimulation parameters. The entire cost for the device was less than \$40 which could be reduced even further if the device was to be produced in larger quantities. This device was extensively bench tested prior to use with cells. The results of this bench testing indicated that the device could successfully regulate the output up to 250 mA and a voltage could be reliably selected with greater than 1% accuracy.

2.6. System to integrate stimulation into cell cultures

To integrate the electrical stimulation and the cell culture scaffolds, a system was developed. The protocol described in Tandon, et al. [22] was used as the basis for the design of this system. This protocol recommends affixing carbon rod electrodes in parallel on the base of a petri-dish using silicone rubber. Carbon rods were used due to their biocompatibility, low price and high resistance to corrosion [26]. Platinum wire was used to connect the carbon electrodes to alligator clips that were connected to the stimulator outputs. Platinum wire was chosen due to its flexibility, biocompatibility and high resistance to corrosion [22].

This system uses 25 mm long, 3 mm diameter graphite rods (Sigma Aldrich) as electrodes, connected to the stimulation device outputs using 0.25 mm diameter platinum wire (Sigma Aldrich). A 0.5 mm hole was drilled into each rod, 5 mm from the end. On each rod, a 60 mm length of platinum wire was wrapped around and secured using the hole, leaving approximately 40 mm of additional wire for the stimula-

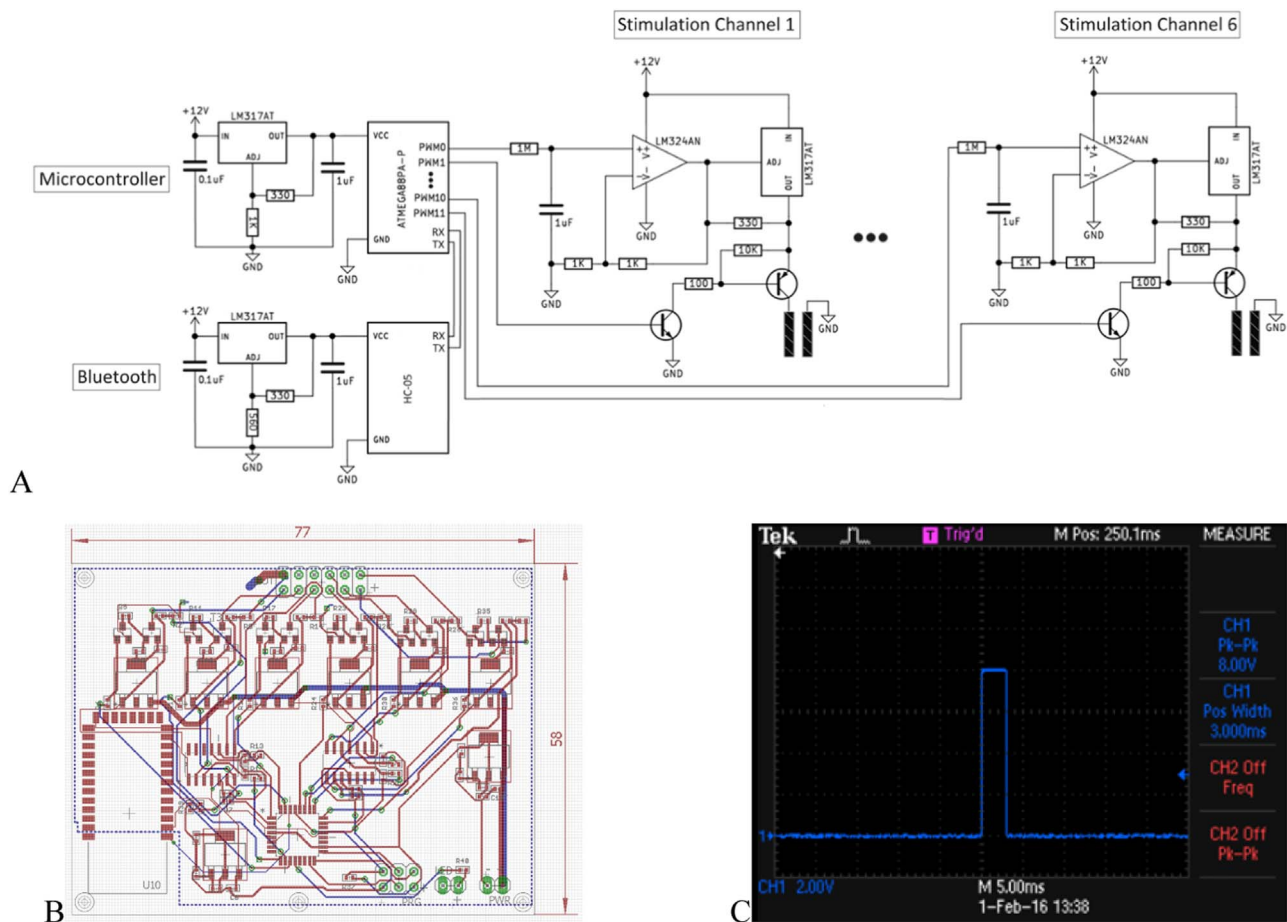


Fig. 3. (A) A diagram of a six channel microcontroller based circuit which produces fully adjustable stimulation pulses, controlled via Bluetooth, for the stimulation of cell culture scaffolds. (B) The layout of the circuit as a Printed Circuit Board (PCB). (C) The output of a bench test producing an 8 V stimulation pulse with a duration of 3 ms.

tion device to be connected. These rods (2 per well) were then secured within a 6-well cell culture plate, 1 cm apart using silicone rubber.

2.7. Cell culture

Adult primary human cardiomyocytes (pHCM) isolated from a male donor, obtained from Celprogen Inc. (San Pedro, CA), and grown up to a maximum of three passages (recommended by Celprogen Inc.), were employed throughout this study. pHCM were cultured in extra cellular matrix (ECM) coated flasks, slides and plates (Celprogen Inc.) in human cardiomyocyte culture complete growth media containing antibiotics (Celprogen Inc.) with 10% foetal bovine serum (Bovogen Biologicals Pty. Ltd.), and maintained at 37 °C in 5% CO₂ both pre and post treatments.

2.8. Cell culture scaffold experimental procedure

In order to determine the suitability of each scaffold type as a platform for pHCM culture, an experiment aimed to compare the cell attachment and differentiation between cells grown on scaffolds fabricated from different materials (silicone rubber or PCL) was conducted. To reduce the risk of contamination, the scaffolds were sterilised, through submersion in 70% ethanol solution for 1 h and then exposed to UV light for 24 h. The scaffolds were then placed into a 48-well cell culture plate and seeded with 10³ cells/scaffold. The cell culture plate was then placed within a cell culture incubator (37 °C, 5% CO₂) (Thomson Scientific). After 72 h of growth, the tests were carried out, following which, the cells were fixed with paraformaldehyde (4%) for 20 min at RT. The scaffolds were then placed on glass slides and

stained for cellular actin (red stain) with Alexa Fluor 594 Phalloidin (Molecular Probes/ThermoFisher Scientific), and with 4',6-diamidino-2-phenylindole (DAPI) for the nuclei (blue stain). These were then imaged using a confocal microscope (Leica TCS SP-5) to observe the pHCM growth.

2.9. Stimulated scaffold experimental procedure

In order to determine the effect of electrical stimulation on pHCM cultured on 3D printed PCL scaffolds, an experiment was devised to compare differentiation markers of cells cultured on electrical stimulated scaffolds to control scaffolds (see Fig. 4). This experiment was conducted on pHCM PCL scaffolds fabricated using the method outlined in Section 2.3. To reduce the risk of contamination, the scaffolds were sterilised by submersion in 70% ethanol solution for 1 h and then exposed to UV light for 24 h. The scaffolds were then placed into a 48-well cell culture plate where the pHCM were seeded onto the scaffolds at 10³ cells/scaffold. The cell culture plates were then placed within a cell culture incubator (37 °C, 5% CO₂) (Thomson Scientific). After the cells had reached their optimal growth on the scaffold, the scaffolds were transferred to a 6-well cell culture plate where they were exposed to electrical stimulus. Half of the scaffolds were then subjected to an electrical stimulation (5 V, 2 ms pulses, 1 Hz) for 3 h. After this period of stimulation, the scaffolds were fixed with paraformaldehyde (4%) for 20 min at RT. The scaffolds were then placed on glass slides and stained using Alexa Fluor 594 Phalloidin (Molecular probes/ThermoFisher Scientific) for the actin (red stain) and 4',6-diamidino-2-phenylindole (DAPI) for the nuclei (blue stain). The scaffolds were then imaged using a confocal microscope (Leica TCS SP-5) to observe the results. A total of

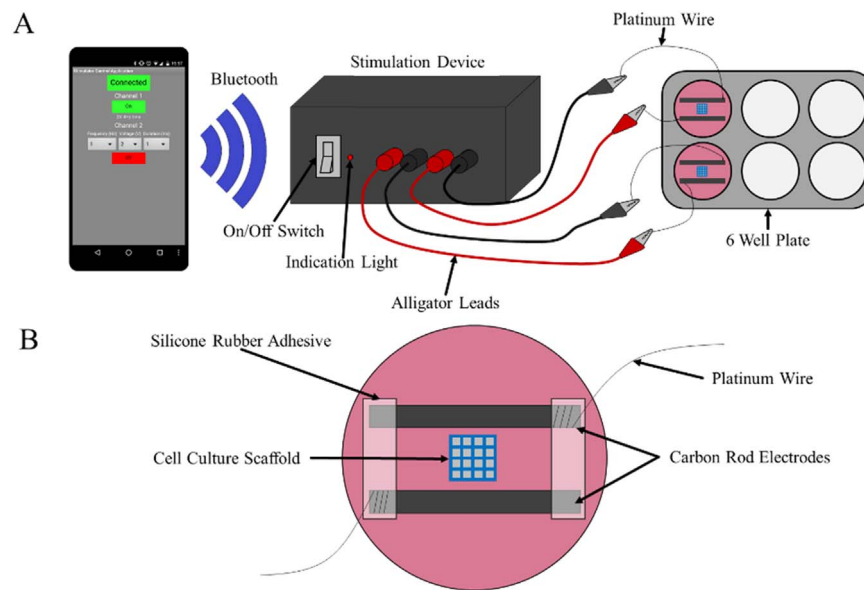


Fig. 4. (A) An illustration of the experimental setup for electrical stimulation test using the custom designed stimulation device. (B) An illustration of a single well of the culture plate showing how the electrical stimulus is delivered to the cell-culture scaffold within the well.

five images were acquired from each treatment to analyse the cells and representative images are given in the results.

2.10. Statistics

All data are expressed as mean \pm SEM. Statistical analyses between the groups were performed with an unpaired Student's *t*-test. A value of $p \leq 0.05$ was considered significant. All bench testing experiments were carried out four times, and all immunoconfocal microscopy experiments were carried out three times and the representative data was presented. For all the laser immunoconfocal microscopy experiments, multiple fields of each treatment were analysed and 100 cells from five fields were counted and the representative images and data are presented.

3. Results and discussion

3.1. Scaffold cell culture experiment

The confocal micrographs of the scaffolds (see Fig. 5A) fabricated using silicone rubber revealed that only a small number of pHCM cells had successfully attached to the printed strands. The attachment of these cells to the silicone strands indicated that the cells remained viable for a period of time in the cell culture environment and that the scaffolds were successfully sterilised. However, after 48 h of culturing only a very small number of the observed cells had attached to the strand and there were no signs of cell migration across the scaffold strand, indicating that the cells were not successfully interacting with the scaffold material.

In comparison, the confocal micrograph images taken of the PCL scaffolds reveal a larger number of pHCM successfully attached to, and interacting with the scaffold strands. The percentage of cells attached in the PCL scaffold was significantly higher (41%) vs. the silicone rubber scaffold (5.3%) ($p < 0.0001$) (see Fig. 5B). In addition, the cells cultured on the PCL scaffolds had migrated across the entire printed strand rather than remaining at the strand boundaries (shown in Fig. 5A & validated through z-stack analysis). These changes indicate that the PCL scaffolds established an environment significantly more conducive to cell viability than those fabricated from silicone rubber.

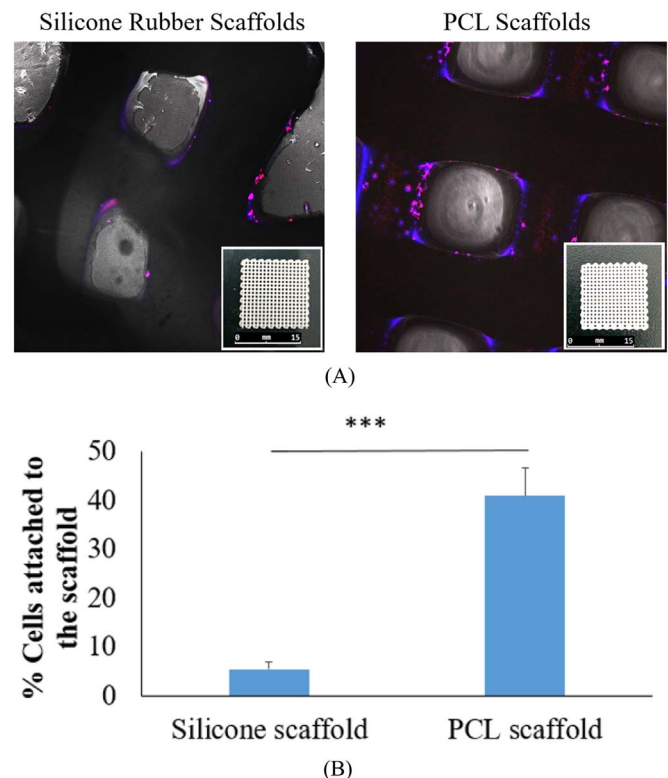


Fig. 5. (A) Fabricated scaffolds, and confocal micrograph images of pHCM cells grown on 3D printed scaffolds (blue nuclei and red actin). (B) Comparison of number of cells successfully attached to the scaffold strands between the scaffolds fabricated from silicone rubber and those fabricated from PCL. $*p \leq 0.0001$ vs. silicone.

3.2. Scaffold stimulation experiment

The bright field micrographs taken as part of this experiment clearly expose a key difference between the stimulated and the unstimulated scaffolds. As can be observed in Fig. 6, the cells in the culture undergoing stimulation were much more closely aggregated towards the scaffold strands, than those in the unstimulated culture. Additionally, there were a higher number of cells observed in the stimulates culture when observed at the same level of magnification.

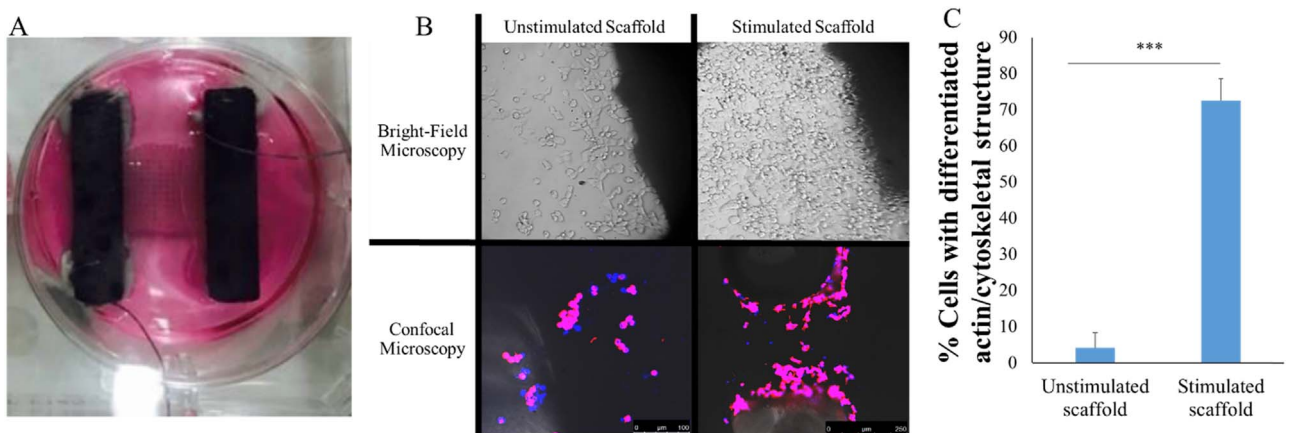


Fig. 6. (A) The experimental setup used to test the effect of stimulation on the pHCM cell cultures. (B) Bright field microscopy image of the base of the culture plate (Grey) and a scaffold strand (Black) of both a stimulated scaffold and an unstimulated control. With confocal images verifying the comparison of average number of cells observed with intact actin structure between the stimulated scaffolds and the control. * $p \leq 0.0001$ vs. unstimulated cells. (C) A graph showing the percentage of cells with differentiated actin structure in both stimulated and unstimulated tests.

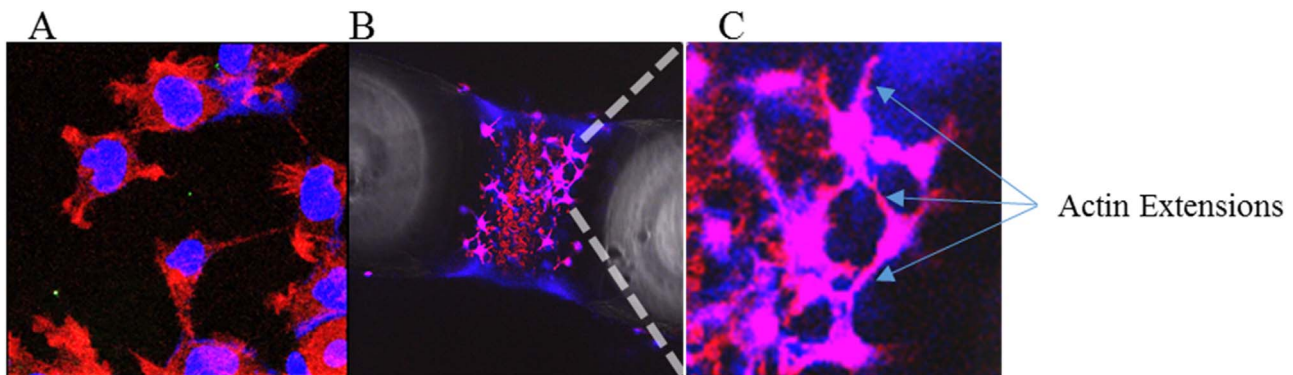


Fig. 7. (A) pHCM successfully grown in a 2D cell culture. (B) pHCM grown on the stimulated PCL scaffold. (C) Magnified section of part B.

The confocal images of both the stimulated and unstimulated cultures (Fig. 6) clearly indicate that cells had successfully attached to the scaffold strands and were beginning migration across the printed strand in both tests. This is in accordance with the results found in Section 3.1, and indicates that the pHCM were successfully interacting with the scaffold material. A large percentage (72.49%) of cells observed in the stimulated test were exhibiting cytoplasmic extensions, indicating possible cellular differentiation. In comparison, only a small percentage (4.17%) of the cells observed in the unstimulated test were exhibiting the cytoplasmic extensions. When compared, it is clear that the cultures undergoing electrical stimulation exhibited significantly more cytoplasmic extensions than those that were unstimulated. This may be due to the stimulation encouraging cell differentiation however, further study using stains with cell differentiation marks would be required to confirm this.

The scaffold also compares favourably to results gathered from a successful 2D primary human cardiomyocyte (pHCM) cell culture, as can be seen in Fig. 7. The 3D cell culture shows the characteristic actin extensions (small extensions away from the nucleus) of a differentiated pHCM; this indicates that the cells are viable and have successfully differentiated in a very similar manner to that seen in successful 2D cell cultures. This indicates that the cells are not only surviving but are growing and are 'healthy'. Also, these images indicate that there is an absence of cell debris on the scaffolds.

4. Conclusions

In this paper, the development and testing of 3D printed pHCM cell culture scaffolds, with and without stimulation using an electrical

stimulation device were described. The primary human cardiomyocytes were isolated from normal human heart (ventricular region), and well characterized by Celprogen Inc. (Catalogue number: 36044-15), and validated by the company by analyzing the expression of cardiac specific markers (ckit, Actinin, ANP, Connexin 43, Desmin, KDR, Nkx2.5, SERCA2, Troponin I, Tropomyosin, MYH6, KCNH2, MYH7, Alpha sacromeric actin). Thereby, these cardiomyocytes were used in the present study [27–29]. Two different scaffold materials (Silicone Rubber & PCL) were tested as platforms for pHCM cell culture. Experimental results indicated that both materials were biocompatible, however, the PCL scaffolds showed more efficacy as there was a higher percentage of cell attachment and more cell migration, compared to the Silicone rubber. The electrical stimulation device, which aimed to be low cost and simple to manufacture, provided electrical stimulation to several cell cultures grown on the PCL scaffolds. This device is controlled by a low-cost android smartphone, and can provide customisable stimulation to multiple scaffolds simultaneously. Using this device to stimulate pHCM cell culture indicated that the efficacy of these scaffolds may be improved by integrating electrical stimulation. Our experiment indicated an increase in cell density in the stimulated cardiac cells in the PCL scaffold as well as an increase in a key differentiation indicator, when compared to a control. However, a further study needs to be carried out using specific cell differentiation markers as to which mechanism is employed by the cells to differentiate into cardiac muscle. Several future work areas have been identified through performing this research including: performing optimisation studies on the scaffold designs, materials, and stimulation parameters for particular cell lines. Furthermore, the proof of concept research presented in this paper should be followed up by investigating different

cellular outcomes, through staining for cell viability or differentiation markers.

References

- [1] J.D. Prince, 3D printing: an industrial revolution, *J. Electron. Resour. Med. Libr.* 11 (2014) 39–45.
- [2] S.V. Murphy, A. Atala, 3D bioprinting of tissues and organs, *Nat. Biotechnol.* 32 (2014) 773–785.
- [3] X. Cui, K. Breitenkamp, M. Finn, M. Lotz, D.D. D'Lima, Direct human cartilage repair using three-dimensional bioprinting technology, *Tissue Eng. Part A* 18 (2012) 1304–1312.
- [4] X. Tao, W.B. Kyle, Z.A. Mohammad, D. Dennis, Z. Weixin, J.Y. James, et al., Hybrid printing of mechanically and biologically improved constructs for cartilage tissue engineering applications, *Biofabrication* 5 (2013) 015001.
- [5] H.-W. Kang, S.J. Lee, I.K. Ko, C. Kengla, J.J. Yoo, A. Atala, A 3D bioprinting system to produce human-scale tissue constructs with structural integrity, *Nat. Biotech.* 34 (2016) 312–319.
- [6] V. Lee, G. Singh, J.P. Trasatti, C. Bjornsson, X. Xu, T.N. Tran, et al., Design and fabrication of human skin by three-dimensional bioprinting, *Tissue Eng. Part C: Methods* 20 (2013) 473–484.
- [7] F. Marga, K. Jakab, C. Khaliwala, B. Shepherd, S. Dorfman, B. Hubbard, et al., Toward engineering functional organ modules by additive manufacturing, *Biofabrication* 4 (2012) 022001.
- [8] A.-V. Do, B. Khorsand, S.M. Geary, A.K. Salem, 3D Printing of Scaffolds for Tissue Regeneration Applications, *Adv. Healthc. Mater.* 4 (2015) 1742–1762.
- [9] B. Duan, State-of-the-art review of 3D bioprinting for cardiovascular tissue engineering, *Ann. Biomed. Eng.* (2016) 1–15.
- [10] K.B. Pasumarthi, L.J. Field, Cardiomyocyte cell cycle regulation, *Circ. Res.* 90 (2002) 1044–1054.
- [11] T. Reffellmann, R.A. Kloner, Cellular cardiomyoplasty—cardiomyocytes, skeletal myoblasts, or stem cells for regenerating myocardium and treatment of heart failure? *Cardiovasc. Res.* 58 (2003) 358–368.
- [12] A. Le Huu, S. Prakash, D. Shum-Tim, Cellular cardiomyoplasty: current state of the field, *Regen. Med.* 7 (2012) 571–582.
- [13] K.L. Christman, A.J. Vardanian, Q. Fang, R.E. Sievers, H.H. Fok, R.J. Lee, Injectable fibrin scaffold improves cell transplant survival, reduces infarct expansion, and induces neovascularization formation in ischemic myocardium, *J. Am. Coll. Cardiol.* 44 (2004) 654–660.
- [14] A.H. Rodney, P.G. Om, Comparison of cardiac-induced endogenous fields and power frequency induced exogenous fields in an anatomical model of the human body, *Phys. Med. Biol.* 43 (1998) 3083.
- [15] F. Pires, Q. Ferreira, C.A.V. Rodrigues, J. Morgado, F.C. Ferreira, Neural stem cell differentiation by electrical stimulation using a cross-linked PEDOT substrate: expanding the use of biocompatible conjugated conductive polymers for neural tissue engineering, *Biochim. Et. Biophys. Acta (BBA) - General Subj.* 1850 (2015) 1158–1168.
- [16] Y.-C. Chan, S. Ting, Y.-K. Lee, K.-M. Ng, J. Zhang, Z. Chen, et al., Electrical stimulation promotes maturation of cardiomyocytes derived from human embryonic stem cells, *J. Cardiovasc. Transl. Res.* 6 (2013) 989–999.
- [17] R. Maidhof, N. Tandon, E.J. Lee, J. Luo, Y. Duan, K. Yeager, et al., Biomimetic perfusion and electrical stimulation applied in concert improved the assembly of engineered cardiac tissue, *J. Tissue Eng. Regen. Med.* 6 (2012) e12–e23.
- [18] H. Park, B.L. Larson, M.E. Kolewe, G. Vunjak-Novakovic, L.E. Freed, Biomimetic scaffold combined with electrical stimulation and growth factor promotes tissue engineered cardiac development, *Exp. Cell Res.* 321 (2014) 297–306.
- [19] M. Radisic, H. Park, H. Shing, T. Consi, F.J. Schoen, R. Langer, et al., Functional assembly of engineered myocardium by electrical stimulation of cardiac myocytes cultured on scaffolds, *Proc. Natl. Acad. Sci. USA* 101 (2004) 18129–18134.
- [20] N. Tandon, A. Marsano, R. Maidhof, L. Wan, H. Park, G. Vunjak-Novakovic, Optimization of electrical stimulation parameters for cardiac tissue engineering, *J. Tissue Eng. Regen. Med.* 5 (2011) e115–e125.
- [21] B. Wang, G. Wang, F. To, J.R. Butler, A. Claude, R.M. McLaughlin, et al., Myocardial scaffold-based cardiac tissue engineering: application of coordinated mechanical and electrical stimulations, *Langmuir* 29 (2013) 11109–11117.
- [22] N. Tandon, C. Cannizzaro, P.-H.G. Chao, R. Maidhof, A. Marsano, H.T.H. Au, et al., Electrical stimulation systems for cardiac tissue engineering, *Nat. Protoc.* 4 (2009) 155–173.
- [23] M.A. Woodruff, D.W. Huttmacher, The return of a forgotten polymer—Polycaprolactone in the 21st century, *Progress. Polym. Sci.* 35 (2010) 1217–1256.
- [24] V.Y. Chakrapani, A. Gnanamani, V. Giridev, M. Madhusoothanan, G. Sekaran, Electrospinning of type I collagen and PCL nanofibers using acetic acid, *J. Appl. Polym. Sci.* 125 (2012) 3221–3227.
- [25] Y. Kim, G. Kim, Collagen/alginate scaffolds comprising core (PCL)–shell (collagen/alginate) struts for hard tissue regeneration: fabrication, characterisation, and cellular activities, *J. Mater. Chem. B* 1 (2013) 3185–3194.
- [26] N. Tandon, C. Cannizzaro, E. Figallo, J. Voldman, G. Vunjak-Novakovic, Characterization of electrical stimulation electrodes for cardiac tissue engineering, in: *Proceedings of the 28th Annual International Conference of the IEEE Engineering in Medicine and Biology Society, EMBS'06, 2006*, pp. 845–848.
- [27] C. Sharma, J.H.S. Satish, R. Rodriguez, M. Sharma, M. Navel, N. Amezcua, et al., Cell based high throughput assay to evaluate cardiovascular safety profile of newly synthesized compounds to be nominated for clinical development, *Mol. Biol. Cell* (2014).
- [28] E.A. Evangelista, R. Kaspera, N.A. Mokadam, J. Jones, R.A. Totah, Activity, inhibition, and induction of cytochrome P450 2J2 in adult human primary cardiomyocytes, *Drug Metab. Dispos.* 41 (2013) 2087–2094.
- [29] A. Ashok, J.R. Kanwar, U.M. Krishnan, R.K. Kanwar, SurR9C84A protects and recovers human cardiomyocytes from hypoxia induced apoptosis, *Experimental Cell Res.* 350 (2017) 19–31.